JOURNAL OF Applied Polymer SCIENCE

Preparation and Characterization of Graphene Oxide/Poly(vinyl alcohol) Composite Nanofibers via Electrospinning

Chen Wang,[1,2] Yadong Li,[1] Guqiao Ding,[2] Xiaoming Xie,[2] Mianheng Jiang[2]

[1]College of Chemistry, Chemical Engineering and Materials Science, Soochow University, Suzhou 215123, China

[2]State Key Laboratory of Functional Materials for Informatics, Shanghai Institute of Microsystem and Information Technology, Chinese Academy of Sciences, Shanghai 200050, People's Republic of China

Correspondence to: Y. Li (E-mail: liyadong@suda.edu.cn) or G. Ding (E-mail: gqding@mail.sim.ac.cn)

ABSTRACT: Graphene oxide (GO) was well dispersed in poly(vinyl alcohol) (PVA) diluted aqueous solution, and then the mixture was electrospun into GO/PVA composite nanofibers. Electron microscopy and Raman spectroscopy on the as-prepared and calcined samples confirm the uniform distribution of GO sheets in the nanofibers. The thermal and mechanical properties of the nanofibers vary considerably with different GO filler contents. The decomposition temperatures of the GO/PVA composite nanofiber dropped by 38–50°C compared with pure PVA. A very small loading of 0.02 wt % GO increases the tensile strength of the nanofibers by 42 times. A porous 3D structure was realized by postcalcining nanofibers in H_2. © 2012 Wiley Periodicals, Inc. J. Appl. Polym. Sci. 000: 000–000, 2012

KEYWORDS: graphene oxide; electrospinning; nanofiber; composite; poly(vinyl alcohol); tensile strength

Received 30 September 2011; accepted 9 March 2012; published online
DOI: 10.1002/app.37656

INTRODUCTION

Nanofiller/polymer composites have been extensively studied due to their wide range of applications. The typical nanofillers include 0D nanoparticles,[1] 1D nanotubes,[2,3] and 2D-layered materials,[4–6] and these materials improve the mechanical, electrical, thermal, and optical properties of the matrix. For the 2D-layered nanofillers, graphite nanoplatelets,[4] mica,[5] and nanoclay[6] are generally used. Graphene (G) and graphene oxide (GO) have very high performances due to high mechanical strength, electrical, and thermal conductivities,[7] making them as the best candidates for nanofillers.[8–12] It has been demonstrated that, with the same loading, the graphene-reinforced composites out-performed significantly in mechanical properties as compared with their counterparts with single-walled/multi-walled carbon nanotubes as nanofillers.[9,13] Thermal stability can also be greatly improved as evidenced by the ~ 30°C increase in glass transition temperature with only 0.05 wt % of graphene in poly(methyl methacrylate).[9]

The general requirements on nanofillers for composites are good homogeneity and interface integrity. The G and GO sheets, if well dispersed in the polymer matrix, may form a highly oriented microstructure or co-continuous networks in polymer, which is the fundamental reason of the changes in mechanical, thermal, and electrical properties of composites. Melt compounding or extrusion techniques are the most common methods in making polymer-based composites. However, they cannot well disperse G or GO in the polymer matrix,[14,15] probably due to the nanofillers' large surface area and incompatibility with the polymer matrix. It is very hard for the molten polymer to fully cover the two-sides of the extremely thin G and GO sheets. The removal of air bubbles trapped in the G and GO sheets during compounding is another major challenge. Obvious agglomerations were evidenced by the presence of graphene stacks with large layer numbers.[14]

Another important approach, which is also widely used in synthesis of polymer-based composites, is solution based,[16–19] that is to dissolve the nanofiller and the polymer matrix in an appropriate solvent. By evaporating the solvent, the composite is made. This method was introduced in the fabrication of G/polymer or GO/polymer composites with success.[20–22] Yang et al.[20] realized GO/poly(vinyl alcohol) (PVA) composite with much improved thermal and mechanical properties. Thick GO/polystyrene composite films were made by Cote et al. with a following flash reduction to realize G/polystyrene composite film.[21] GO/poly(benzimidazole) composites were made by Wang et al.[22] They reported that small GO loading produced

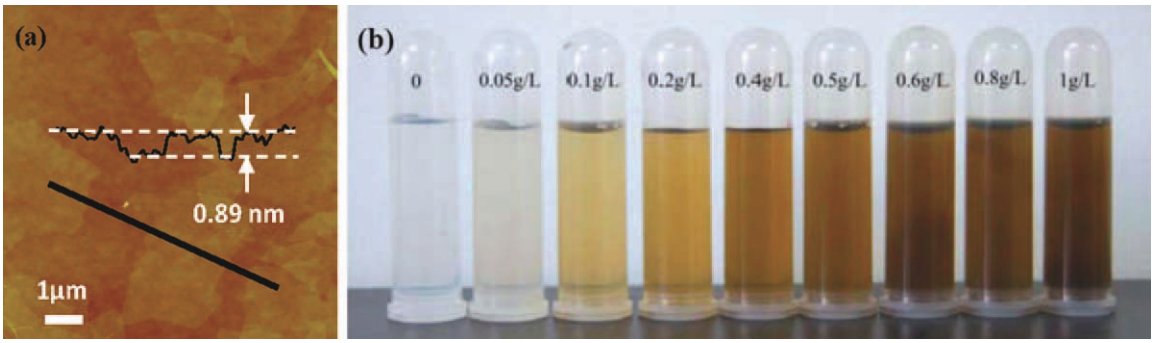

Figure 1. (a) Typical AFM image of GO nanosheets and (b) digital photos of GO/PVA suspensions with various GO concentrations. [Color figure can be viewed in the online issue, which is available at wileyonlinelibrary.com.]

profound effects on the mechanical and thermal properties of the composite. So far, most G/polymer and GO/polymer composites focus on thick films or bulk materials.

Polymer-based composites come in different forms, among which nanofibers are of particular interests due to a big variety of important applications.[10,23] The general fabricating methods of polymer-based composite nanofibers are electrospinning,[10] self-assembly,[24] phase separation,[25] and nanoporous template.[26] The electrospinning process, patented in 1934 by Formhals,[27] is a very important technique for making nanofibers, because of its simplicity and flexibility in producing homogeneous fibers with adjustable diameter and microstructure with various nanofillers. Moreover, the high electrical field present during the spinning process may improve interactions between the nanofiller and the polymer matrix, thus improving the filler/matrix coupling at the interface in molecular scale.

In this report, we disperse GO in PVA aqueous solution to form stable colloidal suspensions, then electrospin to remove solvent and realize GO/PVA nanofibers. The microstructure of nanofibers was characterized, and thermal and mechanical tests demonstrate that the properties of the nanofibers change significantly with GO filler content.

EXPERIMENTAL

Synthesis of GO Sheets and GO/PVA Suspensions

GO was synthesized from graphite using a modified Hummer's method. Briefly, graphite flakes (1.5 g), $NaNO_3$ (1.5 g), and H_2SO_4 (69 mL) were mixed and stirred in an ice-water bath. After that, 9 g $KMnO_4$ was slowly added. The mixture was then allowed to warm to room temperature and stirred for 1 h. Deionized water (100 mL) was added to the solution followed by stirring for 30 min at 90°C. The mixture was poured into 300 mL of water, followed by slowly adding 30% H_2O_2 (10 mL). The reaction mixture was re-dispersed in water and filtered several times until the pH was about 7. Finally, the filtrate was dried in vacuum oven overnight to obtain the GO product. Dried GO was dispersed in water to prepare GO suspensions with different concentrations (0.05–1.0 g/L) with the help of ammonia and mild sonication. At last, 10 wt % PVA aqueous solution [1799, degree of hydrolysis, 99.8%–100% (mol/mol)] was added to the GO dispersion by stirring to form stable GO/PVA suspensions with a ratio of 4 : 1 in the volume of GO suspensions and PVA aqueous solution.

Electrospinning

Typically, ~ 2 mL GO/PVA suspensions was filled in a 5-mL syringe, with a blunt-end, stainless steel needle (inner diameter = 0.711 mm) attached at the open end. The needle was connected to the emitting electrode of a high-voltage supply capable of generating DC voltages in the range of 0–50 kV. A high-purity aluminum foil was used as the collection screen which was connected to the ground electrode of the power supply with the distance between the screen and the needle tip of 12 cm. The electrospinning process was carried out at room temperature. For a GO concentration up to 1.0 g/L, the actual voltages ranged between 9 and 15 kV. To obtain continuous and homogenous nanofiber, the voltages applied were adjusted during the process, whenever necessary, to accommodate variations caused by changes in viscosity, etc. The obtained nanofibers were post-annealed at 500°C under N_2 and H_2 to reduce the GO in the nanofibers.

Characterization

The GO sheets were characterized by atomic force microscopy ((AFM), Veeco, Nanoman VS system with TRESP probe) after spin coating the GO suspension on silicon substrate.

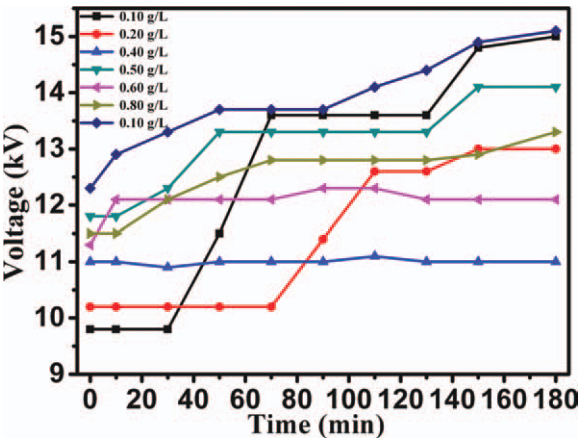

Figure 2. The variation of optimal voltages with time during the electrospinning. [Color figure can be viewed in the online issue, which is available at wileyonlinelibrary.com.]

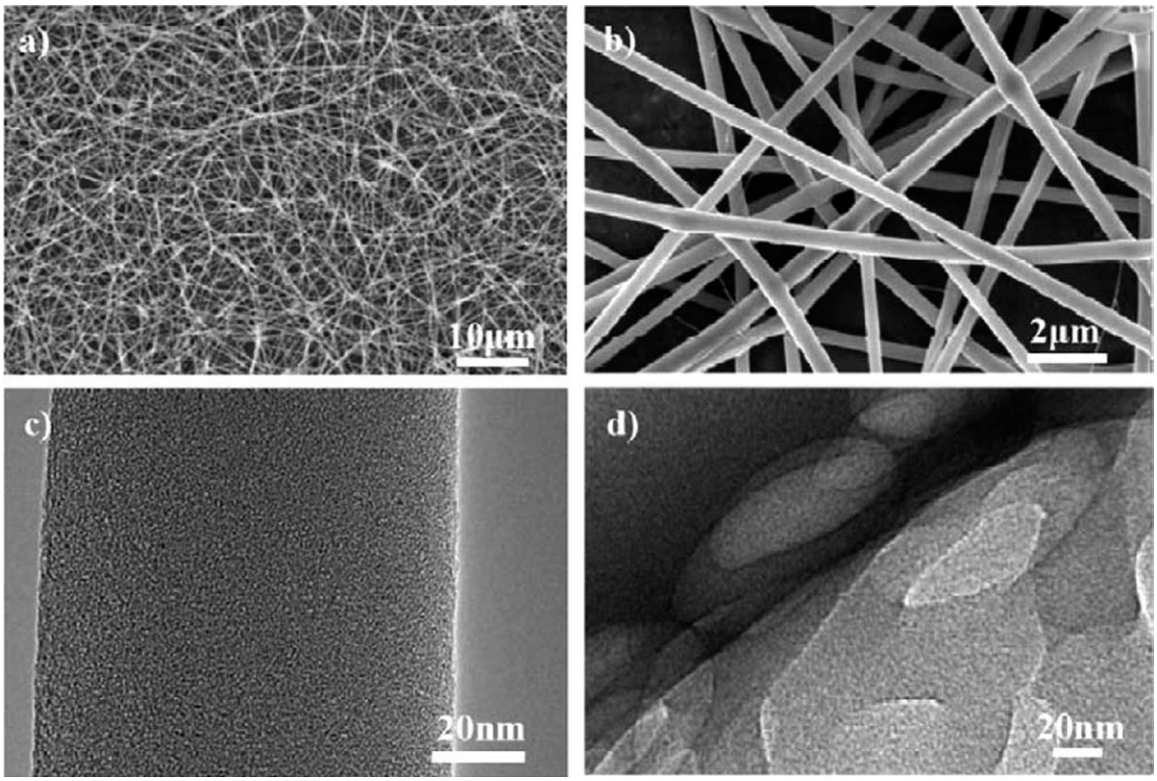

Figure 3. (a,b) Typical FESEM images of GO/PVA nanofibers fabricated by electrospinning. (c,d) Typical HRTEM images of GO/PVA nanofibers.

Morphology of the nanofibers was characterized by a field emission scanning electron microscopy (FESEM; HITACHI S-4700) and high resolution transmission electron microscopy (HRTEM, JOEL JEM2100 under 200 kV). Raman test was performed on Thermo DXR Raman Spectroscopy, with 532 nm laser and 1–5 mW power. Thermogravimetric analysis (TGA) and differential thermogravimetric analysis (DTG) were carried out on a SDT Q600 from TA Instrument under nitrogen atmosphere in the range of 20 to 500°C with a heating rate of 5°C/min. The mechanical test was conducted on a XQ-1A fiber tensile tester according to the literatures.[10,28] The loading rate was 30 mm/min and the load cell was 200 cN with a gauge length of 10 mm. All samples were cut into strips of 30 mm × 5mm. The thickness (150–200 μm) of the mat was measured by micrometer caliper and the nominal cross-section areas of samples were about 0.15–0.2 × 5 mm^2. The diameter of a single nanofiber was estimated by FESEM.[29] The nominal strength (MPa) of the sample was calculated by the loading force (cN) divided by the nominal cross-section area. In all cases, five samples were tested from which the mean and standard deviations were calculated.

RESULTS AND DISCUSSIONS

Stable GO/PVA Suspensions

The obtained GO sheets were characterized by AFM after spin coating on silicon substrates. The typical lateral size is about 1–5 μm, and most of them are single-layered, as shown in Figure 1(a). The addition of ammonia in the GO suspension is very helpful for good exfoliation and dispersion of the GO sheets. As a result, stable GO suspensions can be obtained by mild sonication (40 W) within several minutes. The ammonia can be removed during the electrospinning. The digital photos of different GO/PVA suspensions are shown in Figure 1(b). The marked concentrations refer to the GO suspensions before mixing with PVA aqueous solution. The color becomes deeper as the GO concentration increases. The GO/PVA suspensions are very stable, and there is no sediment or color change after standing for 3 months.

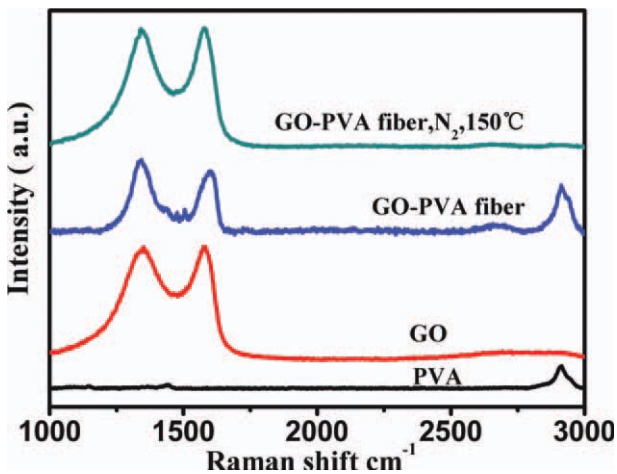

Figure 4. Raman spectra obtained from GO, PVA, and GO/PVA nanofibers. [Color figure can be viewed in the online issue, which is available at wileyonlinelibrary.com.]

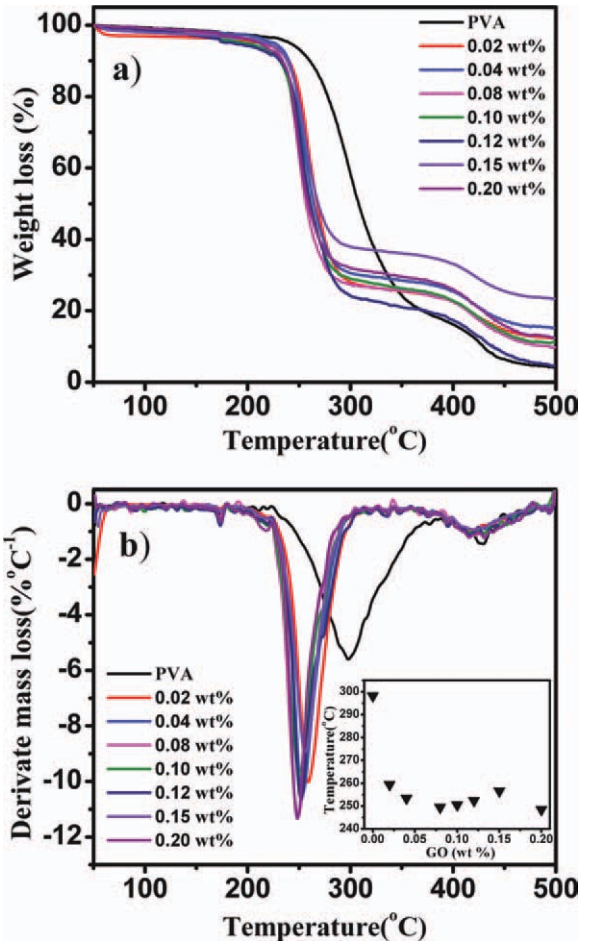

Figure 5. TGA and DTG curves of pure PVA and GO/PVA nanofibers. [Color figure can be viewed in the online issue, which is available at wileyonlinelibrary.com.]

Optimal Voltage During the Electrospinning

Figure 2 shows the variation of optimal voltage with time during the electrospinning process. It shows that we have to adjust the applied voltage to maintain the electrospinning current at a given value (0.02 mA) during the electrospinning process, the applied voltage was called the optimal voltage and the initial optimal voltage increases with increased nanofiller content. At the same time, the optimal voltage increases with time for different nanofiller additions, with the exception of GO suspension content 0.4, where the optimal voltage was quite stable throughout the processes.

The GO sheet has a 2D structure and its lateral size is about 1–5 μm. The single-layer-thick GO may locally restrain the motion of the polymer chains. The sheets are in microns, much larger in size than the nanofibers with a typical diameter of 100–500 nm, which implies a very delicate assembly process. Suspensions with different nanofiller contents will have different viscosity. And for each suspension, the viscosity will also change as solvent volatizes during the processes. The above factors may interact with each other in complicated ways, thus a detailed clarification of the process may not be practicable. However, the material and process parameters can be optimized experimentally.

Nanofiber Morphology

The electrospinning process will remove water and form solid GO/PVA composite nanofibers. The GO content in the nanofibers is about 0.02–0.20 wt % by calculating the net weight of GO and PVA in the nanofibers, respectively. The SEM images of typical GO/PVA nanofibers with GO content of 0.08 wt % are shown in Figure 3(a,b). It can be clearly seen that the as-prepared nanofibers are uniform in diameter and smooth in surface morphology with a diameter of 200 nm on average. In fact, the diameter of obtained non-woven fabric ranges from 100 to 500 nm in our experiment determined by the GO concentrations and the experimental parameters. Most importantly, there were almost no beaded fibers, indicating that the choice of electrospinning parameters is right,[30] and that the GO/PVA mixed suspension is easy to be electrospun. The bright point in Figure 3(a) is the joints of different nanofibers. Figure 3(c) shows a HRTEM image of a typical GO/PVA nanofiber. Unlike reported in the literature,[10] where contrast difference can be seen in the HRTEM images, the image of obtained nanofiber does not show any contrast variation indicating that the composite is very homogenous. Air bubbles are very seldom. Occasionally, in one of the nanofiber with entrapped air, we found the trace of GO sheets. Figure 3(d) showed obvious contrast variation which should be caused by GO sheets inside the nanofiber.

Raman Results

Figure 4 shows the Raman spectra of GO, PVA, and GO/PVA nanofibers before and after calcining under N_2 atmosphere. For the PVA itself, the band with maximum at 2911 cm^{-1} can be attributed to valence C—H vibrations and a band at 1443 cm^{-1} to shear mode. The band at 1143 cm^{-1} serves as a measure of PVA crystallinity.[31] The Raman spectrum of as-prepared GO powder displays a broad D-band at 1340 cm^{-1}, a broad G-band at 1577 cm^{-1}, and a small 2D-band at 2685 cm^{-1}.[32] The G-band and 2D-band shift to 1600 and 2674 cm^{-1} in GO/PVA nanofibers, respectively, which may be relative to the stress between GO and PVA.[33] The typical peaks of GO can be found

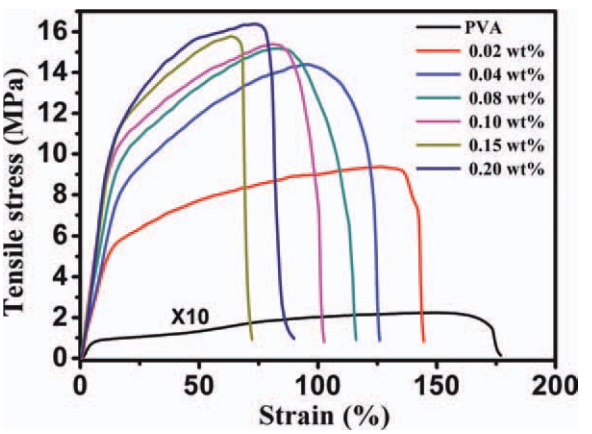

Figure 6. Tensile stress–strain curves of nanofibers with various GO loading. [Color figure can be viewed in the online issue, which is available at wileyonlinelibrary.com.]

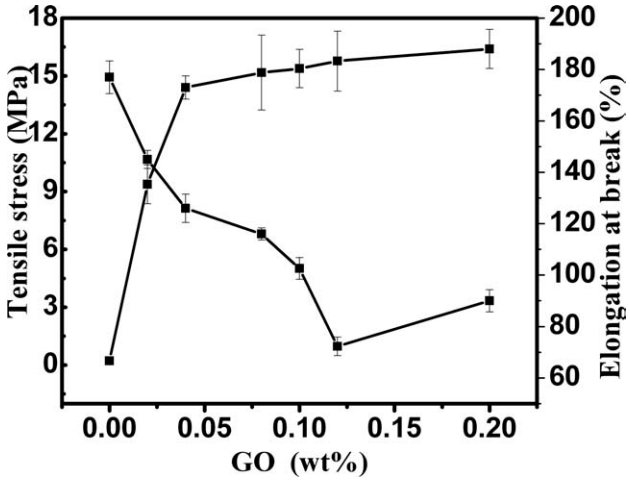

Figure 7. Tensile stress and elongation at break of nanofibers with various GO loading.

in the Raman spectrum of as-prepared and calcined GO/PVA nanofibers, which confirms that the GO survived under the high voltage and electrostatic force, and that the sheets are well distributed in the nanofiber. These results are also consistent with the HRTEM images. After calcining under N_2 at 500°C, the characteristic Raman peaks of PVA disappear due to its pyrolysis, which is in agreement with that reported in Ref. 28.

Decomposition Temperature

TGA and corresponding DTG results for pure PVA and GO/PVA nanofibers with 0.02 to 0.2 wt % GO are shown in Figure 5. The trend for weight loss was the same for all samples. The first loss [$\sim$ 10%, Figure 5(a)] takes place before 200°C, which is mainly ascribed to the removal of adsorbed water and decomposition of labile oxygen functional groups in the material. The main loss over the temperature range of 200–350°C is $\sim$ 50%–70%, which can be assigned to the thermal decomposition of the PVA matrix. The decomposition temperature significantly decreases from 298°C (0% GO) to 248°C (0.2 wt % GO) with the addition of GO nanofillers.

The thermal properties of GO/PVA nanofibers are possibly jointly determined by two competing factors. In one hand, the 2D sp^2 sheet structure of G/GO may act as gas barriers suppressing the decomposition of PVA, resulting in increased decomposition temperature.[8,20,34–36] In Ref. 8, the increase of the decomposition temperature is as high as 36°C when the GO loading is 3 wt % in the GO/PVA composite films. In Ref. 20, 3.5 wt % GO loading increases the decomposition temperature from 270 to 318°C of PVA matrix. On the other hand, when GO undergoes reduction around 200°C,[37] CO, CO_2, and H_2O released during reduction may accelerate the PVA decomposition. Because our samples are nanofibers with diameters of only 100–500 nm, while the typical GO nanofillers curled inside the PVA matrix have a typical size of 1–5 μm, with a extremely large surface area, thus slight outgassing from inside due to GO

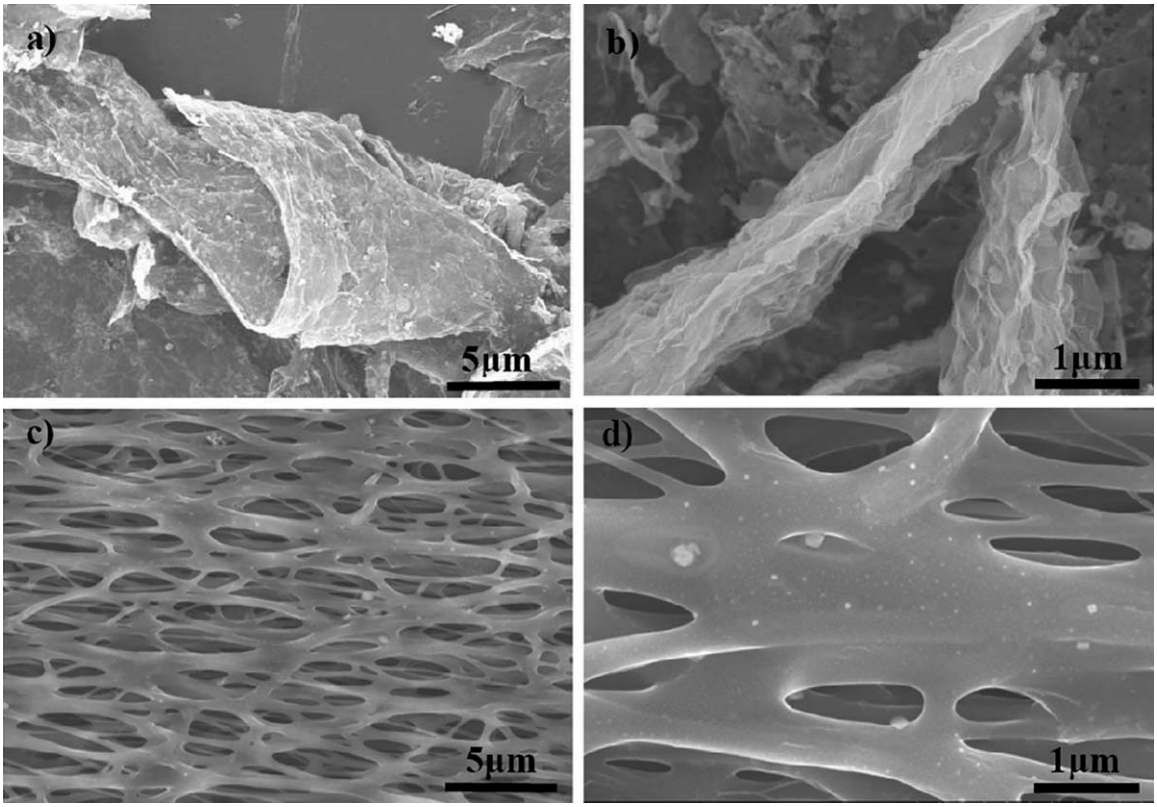

Figure 8. FESEM images of calcined nanofibers, (a,b) under 500°C in N_2, (c,d) 500°C in H_2.

reduction may eventually cause a quick breakdown of the PVA polymer matrix.

Mechanical Properties

Nominal tensile stress–strain tests on the electrospun nanofibers were conducted. The representative stress–strain curves of GO/PVA nanofibers are shown in Figure 6. From the much steeper slope of curves, it is evident that the Young's modules of the GO/PVA nanofibers are significantly increased. The averaged tensile strength and elongation at break of GO/PVA nanofibers are presented in Figure 7. The tensile strength of the GO-loaded PVA nanofiber is increased abruptly by more than one order of magnitude, from 0.22 MPa of pure PVA to 9.37 and 14.39 MPa with 0.02 and 0.04 wt % GO loading, respectively. When more GO is added, the tensile strength gradually saturates. The addition of GO in PVA matrix decreases the elongation at break of the composite. With 0.02 wt % GO loading, the elongation at break dropped to 145% compared with the pure PVA nanofiber with a much higher value of 180%. Higher GO content from 0.04 to 0.2 wt % will cause further decrease in the elongation at break. The effect of GO on the elongation at break can be reasonably attributed to a large aspect ratio and the interaction between GO and the matrix, which restricts the movement of the polymer chains, as proposed by Zhao et al. in Ref. 12.

It is worthy to point out that a very small loading of 0.02 wt % GO increases the nominal tensile strength of the nanofibers 42 times, which is much higher than that of GO/PVA films with much more GO loading.[8,12,20] The electrostatic force during the electrospinning process may improve the interaction between PVA and GO nanofillers, and size-effect in nanofibers may also contribute to the improvement of mechanical properties. These results indicate that the GO or G nanofillers may be utilized for high strength nanofibers.

3D Network Through Postcalcining

Because above measurements and discussions have solidly demonstrated the good distribution of GO sheets in the PVA matrix, we try to remove PVA through postcalcining, and to reduce GO at the same time, to realize GO or graphene nanofiber or other nanostructures. Figure 8 shows the FESEM photographs of the typical GO/PVA nanofibers with GO content of 0.08 wt % after postcalcining at 500°C under N_2 and H_2 atmospheres. The as-prepared composite nanofibers are smooth with nanofiber diameter distribution from 100 to 500 nm. After thermal treatment in N_2, the nanofiber structure collapsed due to the thorough decomposition of PVA matrix. As the GO nanofillers were very thin and its proportion in nanofibers was so small that these GO nanofillers cannot be free-standing. As a result, GO nanofillers self-assembly into stacks with the lateral size of 1–10 μm and thickness of 200–1 μm. The postcalcining process also caused reduction of GO into G as evidenced by the black color and the measured Raman data.

Because the hydrogen can provide a reducing atmosphere, we further postcalcined the GO/PVA nanofibers in pure hydrogen. The color of sample also turned black due to the reduction of GO, but the isolated nanofibers collapsed into a 3D network with 1–5 μm holes, as shown in Figure 8(c,d). Precipitates are observed on the otherwise smooth surface. The reduced graphene on the top surface likely wrapped itself into sphere to for energy minimization. The 3D porous structure of the nanofibers may find potential applications for filtrations and catalyst carriers in the future.

CONCLUSIONS

We have demonstrated the feasibility of fabricating GO/PVA composite nanofibers by electrospinning with GO loading from 0.02 to 0.2 wt %. The diameter of nanofibers ranges from 100–500 nm. The GO nanofillers were homogenously dispersed in the polymer matrix according to the FESEM, HRTEM, and Raman results. The decomposition temperature of obtained nanofibers decreases with the addition of GO. A small loading of 0.02 wt % GO increases the nominal tensile strength of the nanofibers 42 times. A 3D porous network structure was obtained by calcining composite nanofibers in H_2 under 500°C.

ACKNOWLEDGMENTS

This work was supported by projects from NSFC (Grant No. 11104303), Shanghai Science and Technology Commission (Grant No. 10DJ1400600), and the National Science and Technology Major Project (Grant No. 2011ZX02707).

REFERENCES

1. Zhang, D.; Karki, A. B.; Rutman, D.; Young, D. P.; Wang, A.; Cocke, D.; Ho, T. H.; Guo, Z. *Polymer* **2009,** *50*, 4189.
2. Sui, X. M.; Giordani, S.; Prato, M.; Wagner, H. D. *Appl. Phys. Lett.* **2009,** *95*, 233113.
3. Sui, X. M.; Wagner, H. D. *Nano Lett.* **2009,** *9*, 1423.
4. Quan, H.; Zhang, B. Q.; Zhao, Q.; Richard, K. K. Y.; Robert, K. Y. L. *Composites A.* **2009,** *40*, 1506.
5. Khan, A. N.; Hong, P. D.; Chuang, W. T.; Shih, K. S. *Mater. Chem. Phys.* **2010,** *119*, 93.
6. Bilotti, E.; Zhang, R.; Deng, H.; Quero, F.; Fischer, H. R.; Peijs, T. *Compos. Sci. Technol.* **2009,** *69*, 2587.
7. Soldano, C.; Mahmood, A.; Dujardin, E. *Carbon* **2010,** *48*, 2127.
8. Xu, Y.; Hong, W.; Bai, H.; Li, C.; Shi, G. *Carbon* **2009,** *47*, 3538.
9. Ramanathan, T.; Abdala, A. A.; Stankovich, S.; Dikin, D. A.; Herrera-Alonso, M.; Piner, R. D.; Adamson, D. H.; Schniepp, H. C.; Chen, X.; Ruoff, R. S.; Nguyen, S. T.; Aksay, I. A.; Prud'Homme, R. K.; Brinson, L. C. *Nat. Nanotechnol.* **2008,** *3*, 327.
10. Bao, L. Q.; Zhang, H.; Yang, J. X.; Wang, S.; Tang, D. Y.; Jose, R. *Adv. Funct. Mater.* **2010,** *20*, 782.
11. Wu, Q.; Xu, Y. X.; Yao, Z. Y.; Liu, A.; Shi, G. Q. *ACS Nano* **2010,** *4*, 1963.
12. Zhao, X.; Zhang, Q.; Chen, D.; Lu, P. *Macromolecules* **2010,** *43*, 2357.
13. Rafiee, M. A.; Rafiee, J.; Wang, Z.; Song, H. H.; Yu, Z. Z.; Koratkar, N. *ACS Nano* **2009,** *3*, 3884.
14. Steurer, P.; Wissert, R.; Thomann, R.; Mülhaupt, R. *Macromol. Rapid. Commun.* **2009,** *30*, 316.

15. Kim, H.; Kobayashi, S.; Abdur Rahim, M. A.; Zhang, M. J.; Khusainova, A.; Hillmyer, M. A. *Polymer* **2011,** *52*, 1837.
16. Vanin, A. F. *Nitric Oxide: Biol. Chem.* **2009,** *21*, 1.
17. Jang, Y. K.; Won, J. C.; Yoon, H. G. *Appl. Phys. Lett.* **2009,** *95*, 052907.
18. Kang, L. I.; Gao, Y. F.; Luo, H. *J. ACS. Appl. Mater. Inter.* **2009,** *1*, 2211.
19. Mansurova, S.; Meerholz, K.; Sliwinska, E.; Hartwig, U.; Buse, K. *Phys. Rev. B* **2009,** *79*, 174208.
20. Yang, X. M.; Shang, S. M.; Li, L. A. *J. Appl. Polym. Sci.* **2011,** *120*, 1355.
21. Cote, L. J.; Rodolfo, C. S.; Huang, J. X. *J. Am. Chem. Soc.* **2009,** *131*, 11027.
22. Wang, Y.; Shi, Z. X.; Fang, J. H.; Xu, H. J.; Yin, J. *Carbon* **2011,** *49*, 1199.
23. Beachley, V.; Wen, X. *J. Prog. Polym. Sci.* **2011,** *35*, 868.
24. Hong, Y.; Legge, R. L.; Zhang, S.; Chen, P. *Biomacromolecules* **2003,** *4*, 1433.
25. Gong, J.; Uchida, T.; Yamazaki, S.; Kimura, K. *Macromol. Chem. Phys.* **2010,** *211*, 2226.
26. Tao, S. L.; Desai, T. A. *Nano Lett.* **2007,** *7*, 1463.
27. Formhals, A. U.S. Pat. 1,975,504 (**1934**).
28. Jeong, J. S.; Moon, J. S.; Jeon, S. Y.; Park, J. H.; Alegaonkar, P. S.; Yoo, J. B. *Thin Solid Films* **2007,** *12*, 5136.
29. Patra, S. N.; Bhattacharyya, D. *Process. Fabrication Adv. Mater. XIX.* **2011,** *14*, 803.
30. Patra, S. N.; Easteal, A. J.; Bhattacharyya, D. *J. Mater. Sci.* **2009,** *44*, 647.
31. Prosanov, I. Y.; Matvienko, A. A. *Phys. Solid State* **2010,** *52*, 2203.
32. Yang, D.; Velamakanni, A.; Bozoklu, G.; Park, S.; Stoller, M.; Piner, R.; Stankovich, S.; Jung, I.; Field, D.; Ventricejr, C. *Carbon* **2009,** *47*, 145.
33. Lachman, N.; Bartholome, C.; Miaudet, P.; Maugey, M.; Poulin, P.; Wagner, H. D. *J. Phys. Chem. C* **2009,** *113*, 4751.
34. Kim, H.; Miura, Y.; Macosko, C. W. *Chem. Mater.* **2010,** *22*, 3441.
35. Bunch, J. S.; Verbridge, S. S.; Jonathan, S. A.; Arend, M. Z.; Parpia, J. M.; McEuen, P. L. *Nano Lett.* **2008,** *8*, 2458.
36. Kim, H.; Abdala, A. A.; Macosko, C. W. *Macromolecules* **2010,** *43*, 6515.
37. Lu, G.; Ocola, L. E.; Chen, J. *Nanotechnology* **2009,** *20*, 445502.